Motion adaptation improves acuity (but perceived size doesn't matter)

Selassie Tagoh School of Optometry & Vision Science, The University of Auckland, Auckland, New Zealand

Lisa M. Hamm School of Optometry & Vision Science, The University of Auckland, Auckland, New Zealand

Dietrich S. Schwarzkopf School of Optometry & Vision Science, The University of Auckland, Auckland, New Zealand; Department of Experimental Psychology, University College London, London, UK

Steven C. Dakin School of Optometry & Vision Science, The University of Auckland, Auckland, New Zealand; UCL Institute of Ophthalmology, University College London, London, UK

Recognition acuity—the *minimum size* of a high-contrast object that allows us to recognize it—is limited by optical and neural elements of the eye and by processing within the visual cortex. The *perceived size* of objects can be changed by motion-adaptation. Viewing receding or looming motion makes subsequently viewed stimuli appear to grow or shrink, respectively. It has been reported that resulting changes in perceived size impact recognition acuity. We set out to determine if such acuity changes are reliable and what drives this phenomenon. We measured the effect of adaptation to receding and looming motion on acuity for crowded tumbling-T stimuli (⊤ ⊣ ⊥ ⊢). We quantified the role of crowding, individuals' susceptibility to motion-adaptation, and potentially confounding effects of pupil size and eye movements. Adaptation to receding motion made targets appear larger and improved acuity (–0.037 logMAR). Although adaptation to looming motion made targets appear smaller, it induced not the expected decrease in acuity but a modest acuity *improvement* (–0.018 logMAR). Further, each observer's magnitude of acuity change was not correlated with their individual perceived-size change following adaptation. Finally, we found no evidence that adaptation-induced acuity gains were related to crowding, fixation stability, or pupil size. Adaptation to motion modestly enhances visual acuity, but unintuitively, this is dissociated from perceived size. Ruling out fixation and pupillary behavior, we suggest that motion adaptation may improve acuity via incidental effects on sensitivity—akin to those arising from blur adaptation—which shift sensitivity to higher spatial frequency-tuned channels.

Introduction

Recognition acuity

The most common clinical measure of visual function is *recognition acuity*. Assessment of recognition acuity requires an observer to identify high-contrast targets (typically letters) of different sizes (Jackson & Bailey, 2004). The angular size of the smallest identifiable target (at a predefined level of performance) is the observer's recognition acuity threshold. Excellent recognition acuity requires a number of simpler visual subprocesses to be operating at peak performance. Thibos and Bradly (1993) describe these visual subprocesses in a three-stage hierarchical model—comprising *detection*, *resolution*, and *recognition*—where each is limited by optical, neural, or cortical factors (including limits inherited from preceding stages). That recognition acuity requires all three stages be intact makes it a sensitive method for quantifying functional vision (Thibos & Bradley, 1993). In a healthy visual system, there are fundamental limits on each stage, which we summarize in Table 1 and briefly describe below.

Citation: Tagoh, S., Hamm, L. M., Schwarzkopf, D. S., & Dakin, S. C. (2022). Motion adaptation improves acuity (but perceived size doesn't matter). *Journal of Vision*, *22*(11):2, 1–20, https://doi.org/10.1167/jov.22.11.2.

https://doi.org/10.1167/jov.22.11.2 Received May 8, 2022; published October 4, 2022 ISSN 1534-7362

Physiological limits (acuity type)		Nature of limit	Anatomical spatial limit	Frequency limit (c/deg)
Optics (*detection limiting*)				
Monochromatic aberrations	Astigmatic defocus	Magnitude[a] of residual astigmatic defocus: <0.10 D.	<0.15 µm (Villegas, Alcón, & Artal, 2008)	>900
	Spherical defocus	Magnitude of residual spherical defocus: ~0.25 D.	~0.29 µm (Thibos, Hong, Bradley, & Cheng, 2002)	>500
	Higher-order aberrations (HOAs)	Magnitude of the HOAs (coma, trefoil, spherical aberrations): <0.35 µm and approaches 0.045 µm at 3-mm pupil diameter.	<0.35 µm (Salmon & van de Pol, 2006; Villegas, Alcón, & Artal, 2008)	>400
Chromatic aberrations (CAs)	Transverse CA	Magnitude of TCA: ~0.61 arcmin.	3 µm (Thibos et al., 1990)	~82
	Longitudinal CA	Magnitude of LCA: ~1.56 D (0.36 arcmin) across the visible spectrum.	1.8 µm (Thibos et al., 1990)	~50
Pupil	Diffraction	The spatial diameter of the diffraction-limited[b] Airy's disc at a 2.3-mm pupil size[c] is about 0.5–1 arcmin.	~4.94 µm (Campbell & Gubisch, 1966; O'Brien, 1951)	~30–60
Neural limits: Retina/geniculate *(resolution limiting) and* visual cortex *(recognition limiting)*				
Cone cells (fovea)	Density, spacing,[d] aperture[e]	Peak cone density of ~164 K–199 K cones/mm^2, center-to-center spacing of ~2.7 µm, and an aperture of ~1.6–2.2 µm.	~2.7 µm (Curcio, Sloan, Kalina, & Hendrickson, 1987; Wells-Gray, Choi, Bries, & Doble, 2016)	~55
Retinal ganglion cells and LGN[f]	Receptive field size	The smallest RF size of midget-RGCs is ~1 arcmin.	~5 µm (Dacey, 1993)	~30
Central V1 cortical neurons	Receptive field size[g]	Cells have RF sizes of ~4–5 cones wide but have a preferred stimulus width of ~2–3 cones wide (0.7–1 arcmins).	~3.4–5.1 µm (Dow, Snyder, Vautin, & Bauer, 1981)	~30–43

Table 1. How different elements of the visual system limit visual acuity.

[a]For an optical system fully corrected for astigmatism and defocus excluding the effects of other factors such as diffraction and at a 6-mm pupil diameter.

[b]In a perfect diffraction-limited optical system, the cutoff frequency given as 1.22*λ/aperture size is about 60 c/deg for an optical system of focal length 17 mm with light of a 550-nm wavelength. The point spread function for this optical system will have a diameter of about 1 arcmin at half height.

[c]At pupil diameters of between 2 and 3 mm, the effects of aberrations and diffraction are approximately balanced.

[d]The Nyquist limit of the foveal cone mosaic is about 60–85 c/deg.

[e]A smaller cone aperture dictates finer sampling resolution of the cone mosaic.

[f]Lateral geniculate nucleus (LGN) ganglion cells number about 1.2 M cells/mm^2 in humans. Receptive field (RF) properties in the LGN are similar to retinal ganglion cells (RGCs). P (midget) ganglion cells project to the four dorsal layers of the LGN and are responsible for high-acuity performance.

[g]Receptive field size of central cortical neurons is smaller but more numerous while those representing the peripheral field are larger but less numerous, contributing to a higher foveal cortical magnification, a limiting factor for vernier and other forms of hyperacuity such as recognition acuity.

Limits on recognition acuity

Naturally occurring irregularities in the optics of the eye lead to diffraction and aberration of the visual scene (Thibos, Hong, Bradley, & Cheng, 2002; Villegas, Alcón, & Artal, 2008), together limiting the highest spatial frequency that reaches the retina to ~30–50 c/deg (Campbell & Green, 1965). This can be increased to ~60 c/deg by using laser interferometry to bypass such optical limits (Campbell & Green, 1965). At the retina, sampling theory (Shannon, 1948; Snyder & Miller, 1977) suggests cone spacing limits the

highest spatial frequency sinusoidal grating that can be faithfully reconstructed from the cone lattice. This is called the "Nyquist" limit and is around 60 c/deg (Campbell, & Green 1965; Williams & Coletta, 1987).

Although the Nyquist limit constrains resolution acuity (our ability to resolve two objects as being distinct), there are several examples where behavioral performance on other acuity tasks exceeds optical and retinal limits (Campbell & Green, 1965; Levi, Klein, & Aitsebaomo, 1985; Levi, Klein, & Carney, 2000; Thibos, Walsh, & Cheney, 1987; Waugh, Levi, & Carney, 1993; Williams, 1985, 1986; Williams & Coletta, 1987). Recognition acuity (described above) and Vernier acuity (the smallest detectable offset in position) reflect cortical (Hou, Kim, & Verghese, 2017; Levi, Klein, & Aitsebaomo, 1985) rather than retinal or optical limits.

Cortical magnification (CM)—the amount of visual cortex devoted to representing 1 deg of visual space—likely limits some classes of hyperacuity. Although the receptive fields of foveal cells in the retina, LGN (lateral geniculate nucleus), and cortex are small (Kolb, Linberg, & Fisher, 1992; Smith, Singh, Williams, & Greenlee, 2001; Watson, 2014), a higher proportion of cells in the primary visual cortex (V1) respond to foveal than to peripheral input (Connolly & Van Essen, 1984; Curcio & Allen, 1990; Perry & Cowey, 1985), which supports higher cortical magnification for centrally presented targets (Cowey & Rolls, 1974). Boynton and Duncan (2002) found that observers with larger cortical magnification had better Vernier acuity but not resolution acuity. Brain imaging studies on the acuteness of position and orientation resolution suggest a dependence on cortical surface area (Song, Schwarzkopf, Kanai, & Rees, 2015; Song, Schwarzkopf, & Rees, 2013), indicating that CM might play a role in other forms of hyperacuity, like recognition acuity.

The physiological basis of CM is well understood and can be used to model acuity for isolated letters presented in the periphery (Virsu, Näsänen, & Osmoviita, 1987). However, more complex stimuli place additional limits on acuity that are unrelated to CM but may still be cortical in nature. In particular, identification of objects can deteriorate when distracting/irrelevant elements fall too close to them (a phenomenon known as *crowding*; Levi, 2008). Crowding is normally studied in peripheral vision, where it can extend over large regions, known as *interference zones* (i.e., the region around a target within which the presence of distractors disrupts recognition; Bouma, 1970). Since interference zones scale with eccentricity E (as E/2; Bouma, 1970), central targets (where interference zones span only ∼0.75–1.3 arcmin; Coates, Levi, Touch, & Sabesan, 2018) are less susceptible to crowding. In the limit, at the fovea, crowding resembles masking (Levi, Klein, & Hariharan Vilupuru, 2002). Crowding cannot be explained by simple CM in V1, although it has been proposed that it may be explicable by reduced CM in later visual areas such as V4 (Freeman & Simoncelli, 2011).

Optical, retinal, and cortical limits implicitly treat visual scenes as static. However, visual processing is dynamic and factors such as pupil size and eye movements also influence acuity. Pupil diameter changes in response to dynamic lighting as well as attention (Beatty & Wagoner, 1978) and the type of visual information being viewed (Castellotti, Francisci, & Del Viva, 2021; Sahraie & Barbur, 1997, Beukema, Olson, & Jennings, 2017), directly affecting optical transmission of the stimulus (Atchison, Smith, & Efron, 1979) and therefore impacting all forms of acuity. Images are also constantly in motion over the retina, as the combined result of physical object movement and of the oculomotor response of the visual system. Such eye movements are required for observers to achieve high levels of performance with high spatial frequency stimuli (preventing eye movements is detrimental to acuity; unstable fixation eye movements cause blur and reduce acuity; Packer & Williams, 1992; Steinman & Levinson, 1990; Tarita-Nistor et al., 2009). Specific fixational eye movements seem to influence acuity. Intoy and Rucci (2020) suggest that drift characteristics (including speed and curvature of the trajectory of the eye) combine to shift the sensitivity of visually responsive neurons to higher spatial frequencies, so boosting acuity (Intoy & Rucci, 2020).

Recognition acuity and perceived size

In terms of cortical limits on recognition acuity, it has been claimed that both cortical magnification and crowding rely on *perceived* rather than *physical* size. Functional magnetic resonance imaging research on size perception has shown that changes in perceived size, induced by size illusions, reflect the spatial pattern of V1 neuronal activity in humans (Fang, Boyaci, Kersten, & Murray, 2008; Murray, Boyaci, & Kersten, 2006; Schwarzkopf & Rees, 2013; Schwarzkopf, Song, & Rees, 2011). According to these imaging studies, the larger an object appears, the greater its cortical representation. When considering limits on acuity—other than the size of the target—it is interesting to note that for crowding (at least in the periphery), it is the *perceptual* (not physical) separation between target and distracting elements that predicts the extent of visual crowding (Dakin, Greenwood, Carlson, & Bex, 2011).

One way of manipulating perceived size is through motion-adaptation (Whitaker, McGraw, & Pearson, 1999). Prolonged viewing of unidirectional motion causes a static image to appear to move in the opposite direction (motion aftereffect [MAE]; Anstis, Verstraten, & Mather, 1998; Wohlgemuth, 1911). Adapting to receding motion leads subsequently presented objects to loom and appear larger, while adapting to looming

motion leads a subsequently presented target to recede and appear smaller.

Lages, Boyle, and Jenkins (2017) presented evidence for a small but reliable improvement in recognition acuity—specifically, reading strings of crowded letters—following adaptation to receding motion and inconclusive results for acuity decrease following adaptation to looming motion. The authors conclude that acuity can be changed by manipulating the perceived size of targets. If (a) direction matters, and (b) motion adaptation is a predominantly cortical phenomenon (Whitney et al., 2003), then the authors speculate that cortical representation (magnification and minification) of the target drives the phenomenon rather than direction-independent phenomena, such as blur adaptation. The authors' analysis of the effect of letter position (observers were asked to read lines of letters, so letters presented centrally were maximally crowded while those at the ends were minimally crowded) suggested any crowding effects were independent of acuity change. They also largely ruled out pupil size as a confounding variable.

Here we set out to better understand the link between perceived size and acuity, as well as specifically to explore the mechanism that supports adaptation-induced changes in acuity. While our paradigm was guided by Lages et al. (2017), we made several changes to their experimental design in an effort to improve the reliability and sensitivity of the psychophysical measure. Notably:

- We used a different target and task. While Lages and colleagues (2017) had participants read standard crowded Sloan optotypes (i.e., participants performed a 10AFC (ten alternative forced choice) recognition task), we used a Tumbling "T" optotype and a 4AFC orientation discrimination task. Our "T" optotypes are more similar in legibility to one another than the 10 Sloan optotypes (Hamm, Yeoman, Anstice, & Dakin, 2018) and are widely used in crowding experiments as a better controlled proxy task for letter recognition (Dakin, Cass, Greenwood, & Bex, 2010; Whitney & Levi, 2011).
- Our acuity target changed over time, whereas Lages et al. (2017) used a static target. Below we describe how we did this to force observers to only make their judgment when the aftereffect had been given time to build up, in order to maximize the sensitivity of our paradigm to detect change in acuity.
- The row of five Sloan optotypes presented by Lages et al. (2017) was surrounded by a Voronoi pattern—a series of black lines on a white background. We presented a row of three tumbling Ts and did not include these lines. We did this so we could control *crowding* (in one of our conditions, we presented the targets in isolation). It is, however, possible that the black lines served as a "carrier," allowing the MAE to extend over a larger area. To preempt our findings, however, Experiment 2 quantifies the MAE elicited and shows that it is large.
- The Lages et al. (2017) study used a spiral motion adaptor while we used a concentric-rings motion adaptor. The more complex spiral adaptor may affect a wider range of spatial-temporal motion detectors (Bex, Metha, & Makous, 1999).
- We, unlike Lages et al. (2017), used 4-s top-up adaptation, following the initial 30-s adaptation period. Top-ups are critical in ensuring that the MAE does not decay before observers make their final judgment.

Using our modified paradigm, we aimed to test the hypotheses that (1) adaptation to receding motion improves acuity, and (2) adaptation to looming motion impairs acuity. Despite the differences in experimental design, we report acuity change (Experiment 1) similar to the effect reported by Lages et al. (2017). Acuity gains following adaptation are modest but robust, and it seems unlikely therefore that differences in experimental design between our work and that of Lages et al. (2017) had any significant impact on the conclusions we can draw here. Our experiments also explored whether individual changes in perceived size correlated with changes in acuity (Experiment 2) and whether crowding (Experiment 1) and pupil size or eye movements (all Experiment 3) were likely to account for acuity changes.

General methods

Observers

We recruited 59 participants (28 males, 31 females, 14–56 years, all but 7 naive to the purpose of the experiment) from the University of Auckland staff and student body to participate in Experiment 1 and Experiment 2. All these participants took part in both Experiments 1 and 2. We recruited 30 observers for Experiment 3: 14 from those who took part in Experiments 1 and 2 and 16 new participants. The resulting group comprised 18 males and 12 females, aged 19–52 years, with all but 4 naive to the purpose of the experiment. These sample sizes result from our recruiting within two fixed periods of time for Experiments 1 and 2 and for Experiment 3. Due to coronavirus disease 2019 (COVID-19) restrictions in place at the time of data collection, not all participants could be tested on all conditions of all experiments that they took part in (details are given in each experiment section below).

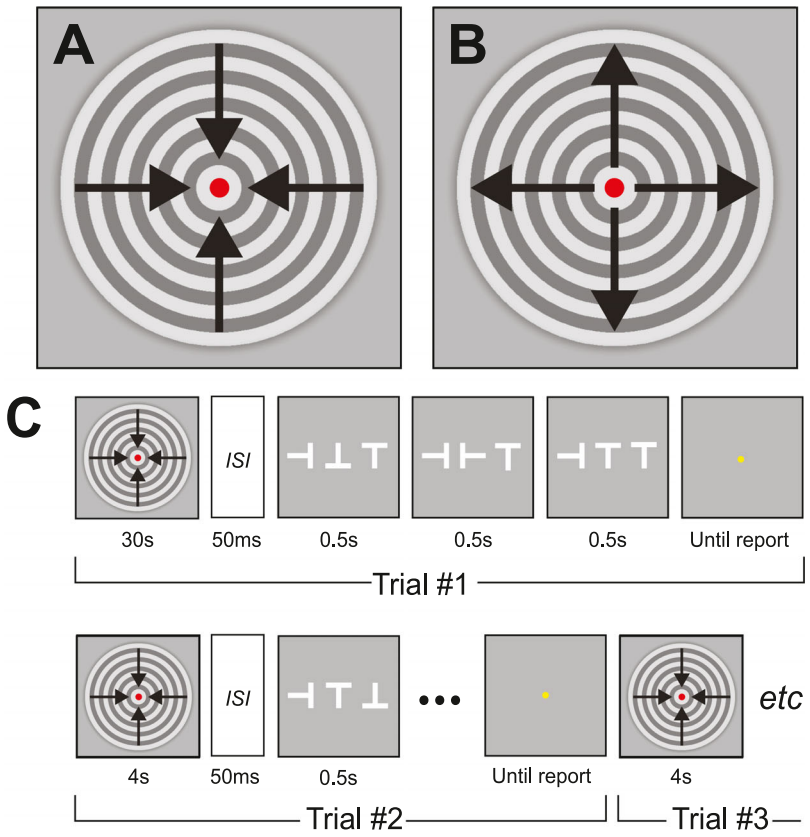

Figure 1. (A) Receding and (B) looming adaptation stimuli. (C) In adapted conditions, participants adapted for either 30 s (first trial) or 4 s (subsequent trials). Following adaptation and a brief ISI, a movie depicting a series of tumbling "T" targets played for 1.5 s. Unadapted conditions were identical except observers did not adapt prior to stimulus presentation. Uncrowded only contained the central "T." For Experiments 1 and 3, observers indicated the orientation of the last "T"-target in the sequence; for Experiment 2, observers indicated whether the target loomed (grew) or receded (shrank).

All observers had (self-reported) normal or corrected-to-normal visual acuity in both eyes. Participants provided informed consent under a protocol approved by the University of Auckland Human Participants Ethics Committee (reference number: 024231). All experiments followed the general tenets and guidelines of the Declaration of Helsinki.

Apparatus

Stimuli were displayed on a 65-in. OLED display (LG 65E6T; LG Electronics Inc., Seoul, South Korea) operating at its native 4K resolution of 3,840 × 2,160 pixels at a screen refresh rate of 60 Hz. The display subtended a visual angle of 11.42 × 20.27 deg at the 4-m viewing distance. The gray background luminance of the display was 67 cd/m^2. Screen gamma was linearized in software using luminance measures made with a photometer (LS100; Konica Minolta, Tokyo, Japan).

Observers were seated in a dimly lit room with their heads supported by a chinrest. They viewed the screen monocularly using their dominant eye.

Stimuli

Experimental stimuli were generated in MATLAB R2019b software (MathWorks Ltd, Natick, MA, USA) using elements of the Psychophysics Toolbox version 3 (Brainard, 1997). Details of the stimulus presentation sequence are given in Figure 1, and an example of a (receding) motion adaptor and crowded target stimuli is shown in Supplementary Movie S1.

The motion adaptation stimulus consisted of a series of high-contrast concentric rings generated as the product of a raised cosine envelope function (radius of 1.24 deg, width of outer band: 0.16 deg) and the sign of a circular sinusoidal function defined as

$$g(d, \lambda, \varphi) = \mathrm{sgn}\left(\cos\left(2\pi\frac{d}{\lambda} + \varphi\right)\right), \quad (1)$$

where d indicates distance from the center, λ is the wavelength of the sinusoid (0.2 deg), and φ is the phase offset (starting at 0 deg increasing/decreasing by 15 deg/frame to generate a movie). The resulting

receding or looming moving circular grating (Figures 1A, B) had a "square-wave" cross section and a duty cycle of 5 c/deg and drifted at 0.5 deg/s.

Throughout adaptation, a 3.0-arcmin diameter red disk served as a fixation point for participants. At the offset of the adaptation stimulus, the fixation marker disappeared (to avoid occluding the target stimulus that followed), and following a 50-ms interstimulus interval (ISI), the stimulus movie appeared. At the end of the stimulus movie, the fixation marker reappeared to indicate that the participant could respond.

The acuity target was a white (134 cd/m^2) "tumbling T," presented at one of four possible orientations (⊤ ⊣ ⊥ ⊢) displayed in the center of a uniform gray background. The target had a 1 to 5 stroke to width ratio, to match Sloan letters. In crowded conditions, the target letter was horizontally flanked by one randomly oriented "T" on each side; the edge-to-edge spacing between target and flanker was 0.5 times the target width. In uncrowded conditions, the target appeared in isolation; note that we only tested uncrowded stimuli without adaptation (to estimate a lower bound on unadapted acuity).

During the 1.5-s stimulus presentation, the target switched orientation three times (Figure 1C), but participants were required to report only its final orientation. Every sequence contained three of the four possible target orientations to avoid repetition. Note that for crowded targets, the flanking Ts did not change orientation during the target stimulus presentation sequence. We changed the target over time so that observers had to wait until the target had assumed its final identity before making a judgment, leaving time for adaptation to build up. This is in contrast to the study by Lages et al. (2017), which allowed for participants to successfully report the identity of a target based on its appearance immediately following offset of the adaptor. As a result, it is possible—in the case of a looming adaptor—that any illusory shrinking effect may not have had time to build up, which may have contributed to inconsistent results for looming motion adaptation.

Psychophysical procedure

For adapted runs (Figure 1C), on the first trial, the adaption stimulus was presented for 30 s, followed by a 50-ms ISI blank, followed by the tumbling-T stimulus. Subsequent trials were similar except the "top-up" adaptor was presented for only 4 s. For acuity tasks (Experiments 1 and 3), observers were required to report—using a computer keypad—the orientation of the tumbling-T target (a 4AFC task). No feedback on their decision was given. The size of the tumbling-T stimulus was set using QUEST, an adaptive staircase procedure (Watson & Pelli, 1983). This procedure concentrated testing at letter sizes eliciting a threshold level of performance (62% correct target identification). The QUEST procedure fits the response-versus-size data with a Weibull function to estimate threshold collected within a single "run" of 35 trials. For each experimental condition, we collected at least three runs for each observer and averaged them together. For the nulling tasks (Experiment 2), the procedure was slightly different. Observers were required to report whether the stimulus appeared to grow or shrink using a computer keypad (a two-alternative task). The magnitude of *physical size change* of the stimulus was set using QUEST (18 trials), which aimed to converge on a physical motion that caused observers to be equally likely to report that the target was growing/shrinking.

We noted on some occasions that staircases failed to converge, which resulted in QUEST producing unreliable size estimates. To minimize the impact of these runs on the pooled estimate, we conducted an outlier analysis on data from each set of runs (3–6) for each participant/condition combination. We considered any set with a standard deviation exceeding 0.1 LogMAR likely to contain an outlier. For sets meeting this criterion, we then determined the run whose exclusion most reduced the estimated standard deviation of the remaining runs and then excluded this run from analysis. We excluded few runs on this basis; between Experiments 1 and 2, only 20 of 1,353 runs (<1.5%) were excluded, and in Experiment 3, 5 of 182 (2.8%) runs were excluded. The slight discrepancy in the proportion of runs excluded is likely attributable to observers becoming less prone to making errors in their response after being tested on a large number of staircases. In Experiments 1 and 2 together, observers were tested on a total of 1,353 staircases, while in Experiment 3, they were tested on only 182 staircases.

The order of runs was randomized, and observers had 2-min breaks between each run (imposed to ensure adaptation effects did not carry over between runs). For each experiment, observers performed at least two practice runs before engaging in the main task. Responses were self-paced, with observers entering their response using a computer keypad when ready. No feedback was provided for any task in any experiment.

Analysis

Analyses were conducted in MATLAB (MathWorks Ltd) and in JASP (JASP Team, 2022) using the Bayesian statistical framework. We relied on repeated-measures analysis of variance (ANOVA), paired *t* tests (directional one-tailed tests in cases where we had a clear prior hypothesis), and Pearson correlation tests (in all cases two-sided tests) to assess whether conditions (specified for each experiment) impacted performance. We exclusively report Bayes factors for the comparisons since the Bayesian framework is flexible w.r.t. (with respect to) differences in sample size (which in our study

arose from the unforeseen end to sampling as a result of COVID-19 restrictions). This framework also enables us to quantify evidence in support of the null hypotheses. The default Cauchy prior in JASP ($r = \sqrt{2}/2$) was used. In terms of the interpretation of results, we used the Bayes factors classification system proposed by van Doorn et al. (2021). According to this classification scheme, the Bayes factors connote the following effects in support of either the null hypothesis: (1–0.33: weak; 0.33–0.1: moderate; 0.1–0.03: strong) or the alternative hypothesis (1–3: weak; 3–10: moderate; 10–30: strong).

Experiment 1: Recognition acuity following motion adaptation

We start by quantifying the phenomenon of interest (acuity change following adaptation to receding or looming motion) using our modified paradigm and determining the role that crowding might play in this effect. Using a within-subjects design, we measured visual acuity for observers who were either unadapted or who had adapted to either receding or looming motion. If acuity changes are driven by perceived size following *receding adaptation*, we would expect acuity *gains* following receding motion adaptation (which makes targets appear to grow). While Lages et al. (2017) reported such an improvement (an average acuity increase of about 0.5 letters across all participants), their rather modest results were prone to ceiling effects, which we mitigated using an adaptive procedure. If acuity changes are driven by perceived size following *looming adaptation*, we would expect acuity *loss* following adaptation to looming motion (which makes targets appear to shrink). Lages et al.'s (2017) results were inconsistent likely because their procedure allowed participants to report stimulus identity before the motion aftereffect had built up. To avoid this, we used a target that changed over time, forcing participants to wait before they reported, which maximizes the aftereffect. We also measured unadapted observers' acuity for *isolated letters*. If acuity gains following adaptation to receding motion are explained by a reduction in the crowding effect of flankers, then by moving flankers away from the target, we expect the following. First, acuity gain from adaptation should be similar to acuity change observed between conditions where flankers are present and absent. Second, observers who are susceptible to crowding should show the largest improvements in acuity following adaptation.

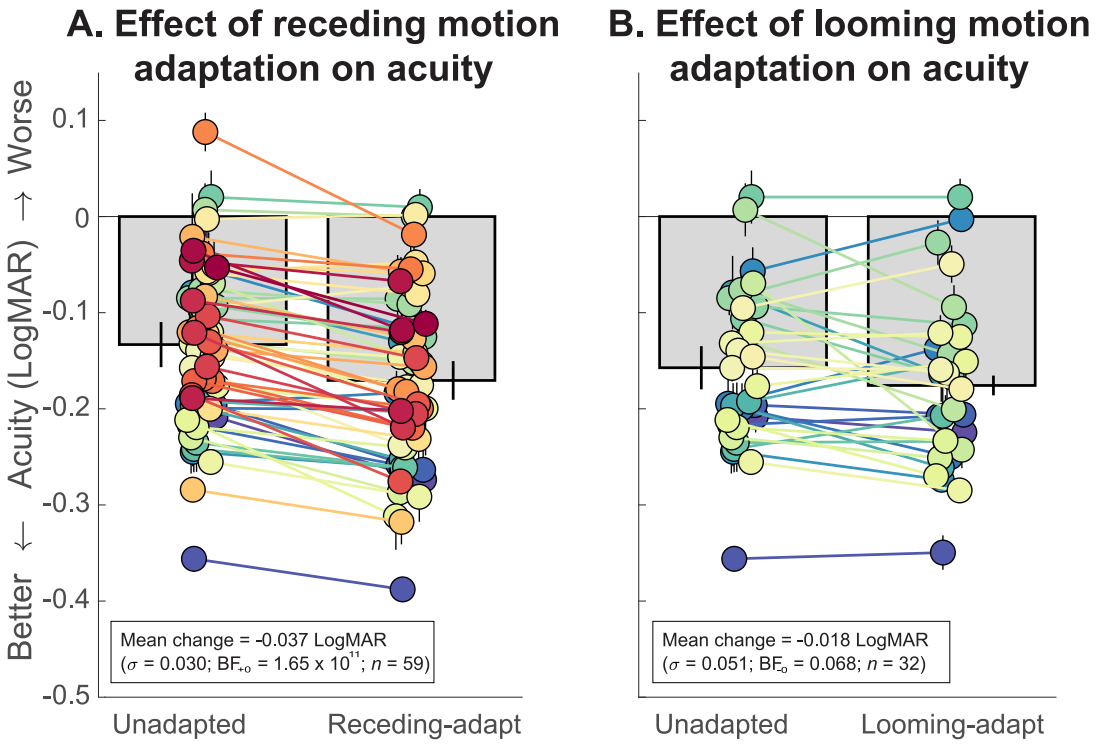

Figure 2. Results from Experiment 1. (A) Crowded visual acuity of observers ($n = 59$) who were either unadapted or who had adapted to receding motion. Gray bars indicate the mean acuity estimate for each condition, and black lines (error bars) denote ± 1 *SEM*. Each pair of colored discs represents data from one observer. (B) is as (A) except observers ($n = 32$) adapted to looming motion. Adaptation to receding motion improves acuity, but adapting to looming motion does not impair acuity. Both adaptation conditions lead to modest but reliable improvements in visual acuity.

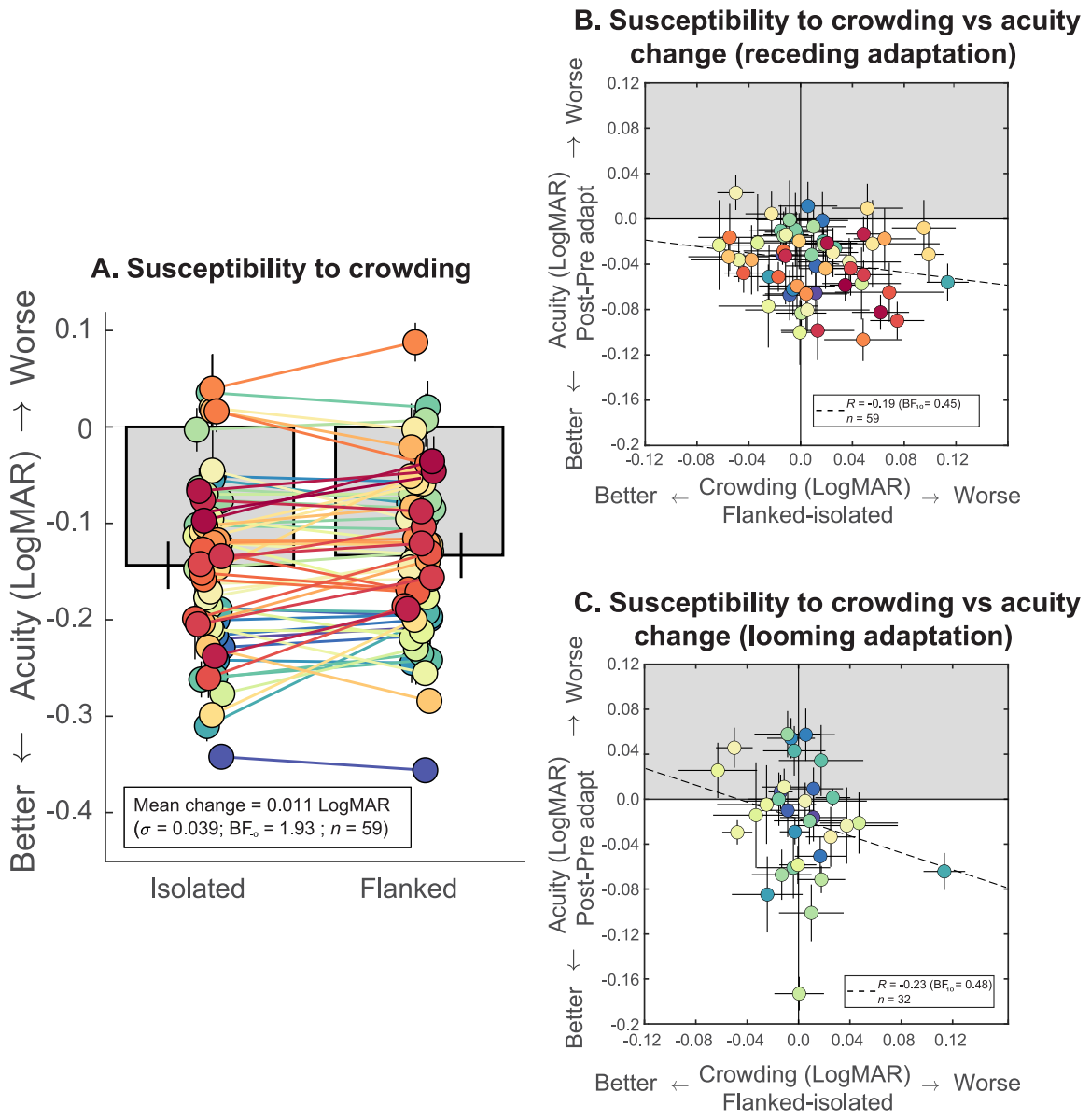

Figure 3. (A) Comparing visual acuity of unadapted observers measured with flanked or isolated targets in Experiment 1 (error bars denote ±1 *SEM*). Mean acuity was slightly better with unflanked (isolated) compared to flanked targets, but the magnitude of this advantage was less than the acuity gains seen following adaptation. (B, C) Individual acuity change (for flanked targets) following adaptation to (B) receding and (C) looming motion plotted against individual susceptibility to crowding (flanked minus isolated acuity without adaptation). Shaded regions indicate a worsening of acuity following adaptation. Our results reveal modest foveal crowding and no associations between acuity change and susceptibility to crowding.

Methods

Fifty-nine observers participated: All took part in three of the four conditions (unadapted crowded letters, receding-adapted crowded letters, unadapted uncrowded letters), but due to COVID-19 restrictions at the time of conducting this study, we were able to secure participation of only 32 of the original 59 observers to complete the fourth condition (looming-adapted crowded letters). We knew that the same participants would be involved in both Experiments 1 and 2, so we sought to recruit as many participants as possible within a fixed recruitment window (February 2020 to June 2021) in order to maximize the sensitivity of our paradigm to detect any underlying correlation between illusion susceptibility and acuity change.

Due to the lack of a prespecified sample size, we employed statistical inference using Bayes factors, which quantifies the statistical evidence for the alternative or null hypothesis given the available data.

Results

Figure 2 plots data showing the impact of motion adaptation on acuity. The results of a repeated measures ANOVA indicate that acuity differed substantially between groups ($F(1.5, 47) = 9.21$, $BF_M = 82.13$). Pairwise directional comparison revealed that this was because adaptation to receding motion induced better acuity than normal (unadapted) viewing conditions (adapted: –0.170 LogMAR, unadapted: –0.133 logMAR, mean gain of –0.037 ± 0.030 LogMAR, $t(58) = 9.71$, $BF_{+0} = 1.65 \times 10^{11}$; Figure 2A). Although the magnitude of acuity gains was variable, adaptation to receding motion improved the acuity of 55 of 59 observers (93%). Such improvement of around 1.85 letters aligns with the results of previous studies (Lages, Boyle, & Jenkins, 2017).[1] When acuity estimates (expressed in LogMAR) were converted to equivalent stimulus sizes, a 3.68-arcmin T could be identified with 62% accuracy without adaptation. After receding motion adaptation, a 3.38-arcmin T (i.e., an 8% smaller stimulus) could be identified with the same accuracy.

Although we expected adaptation to looming motion to make acuity *worse*, results were variable. Sixty-three percent of participants actually showed *acuity gains*, although such changes were an order of magnitude less (mean gain of –0.018 ± 0.051 LogMAR) than for adaptation to receding motion. Comparing mean adapted acuity (–0.175 LogMAR) to unadapted acuity (–0.157 LogMAR) provides strong evidence for the null hypothesis (that looming adaptation does not impair acuity; $t(31) = 2.05$, $BF_{-0} = 0.068$; Figure 2B). This was despite targets (reportedly) being perceived as shrinking and despite our use of targets that were specifically designed to capture acuity losses. We see only weak statistical evidence for there even being a difference between acuity following looming and receding motion adaptation ($BF_{-0} = 1.37$)!

Figure 3 shows the results for the impact of crowding on acuity in Experiment 1. Mean acuity was moderately better with isolated (–0.144 LogMAR) compared to crowded (–0.133 LogMAR) targets (Figure 3A). The mean difference was small (0.011 ± 0.039 LogMAR; $n = 59$), and there were considerable individual differences, but our analysis confirmed a modest foveal crowding effect ($t(58) = -2.05$, $BF_{-0} = 1.93$) as expected. In line with Lages et al. (2017), our results question the role of crowding in this phenomenon in two ways. First, the magnitude of improvement produced by removing flankers is only a quarter of the size of the acuity improvement following adaptation to receding motion. This means that motion adaptation cannot be having its effect wholly through crowding reduction. Second, individual susceptibility to crowding is not associated with acuity changes. Figure 3B,C plots individual susceptibility to crowding (quantified as the individual difference in acuity with crowded and uncrowded stimuli) against acuity change from (Figure 3B) receding and (Figure 3C) looming motion adaptation. Correlation analysis reveals no compelling link between susceptibility to crowding and either receding ($r(59) = –0.19$, $BF_{10} = 0.45$) or looming ($r(32) = –0.23$, $BF_{10} = 0.48$) motion adaptation. It may be argued that we did not observe significant crowding because of the relative dependence of foveal crowding interference zones on target size. This assertion is true assuming that the perceived size of the entire stimulus array changes following adaptation to motion, which predicts that the spatial distances between target and flankers would remain constant and there would be no change in crowding. But this prediction is also subject to the assumption that the change in perceived size following motion adaptation is equally strong across eccentricities, which is unlikely to be the case due to the drop-off in cortical magnification. It is therefore possible that the perceived size of flankers is less strongly affected by motion adaptation than the perceived target flanker distance.

In summary, then, acuity gains following receding motion adaptation cannot be wholly explained by flankers perceptually moving outside interference zones.

Experiment 2: Quantifying susceptibility to motion adaptation

Could the absence of an acuity impairment following adaptation to looming motion be because our motion aftereffect did not cause a reliable perceptual shrinkage of the target? Our original hypothesis, following Lages et al. (2017), rests on the assumption that adaptation leads to a robust change in the perceived size of the target letter. In Experiment 2, we therefore sought to quantify this size illusion directly and to determine if variation in individual participants' acuity gains could be related to how much motion adaptation was affecting their perceptual experience. To this end, we estimated the strength of the receding and looming motion aftereffects, using a motion nulling paradigm that quantifies susceptibility to motion adaptation. Following adaptation to receding motion, we measured how much targets appear to grow or shrink for receding and looming motion adaptation, respectively. If acuity changes are reliant on perceived size, then the magnitude of an individual observer's perceived size change should correlate with their acuity change following adaptation.

Methods

The 59 observers who participated in Experiment 1 also participated in Experiment 2 and were tested on two (unadapted and receding adapted) out of the

three conditions in Experiment 2. As for Experiment 1, only 32 were available for testing on the last condition (looming adaptation).

There are several ways to quantify susceptibility to motion adaptation. One option is to present a reference and ask observers whether the target is larger or smaller than the reference. There are two key issues with this approach: First, the perceived target continues to change over time (the point at which the relative judgment is made likely varies between participants and can include projection based on trajectory), and second, this approach poses physical constraints requiring the target, the reference, or both to be parafoveal (which confounds size perception). We overcame these challenges by presenting adapted observers with targets that either physically shrank or grew in a direction opposite to that of the anticipated motion aftereffect. When the physical change balanced perceptual change, observers experience a target that is stable (for an example, see Supplementary Movie S2).

On each trial, participants were asked to complete a 2AFC decision: whether the target appeared to grow (loom) or shrink (recede). As for all experiments, targets were presented as a 1.5-s movie, with target orientation changing every 0.5 s, and QUEST was used to determine target size. However, in this experiment, the first target in the stimulus sequence was always scaled to 0.14 LogMAR (i.e. a T-height of 6.9 arc min), while the size of the target at the end of the sequence was set by QUEST. The size of elements shown in each frame of the stimulus movie was smoothly interpolated between 0.14 LogMAR and the QUEST scaling for final target size to produce smooth motion. Each QUEST staircase had 18 trials and was designed to converge on a physical motion that caused observers to be equally likely to report that the target was looming/receding. All targets were presented crowded (as in Figure 1). Conditions were: no adaptation, receding motion adaptation and looming motion adaptation. The measure obtained was expressed as the scaling of the 0.14 LogMAR target required to produce a stimulus that was equally likely to be judged to be receding or looming. This scaling was expressed as the logarithm of the scaling value; its units were therefore identical to LogMAR, but we do not label it as such to avoid confusion with acuity measures. The *magnitude* of the illusory effect was calculated as the difference in size change required to null motion in unadapted and adapted conditions.

Results

Figure 4 shows results from Experiment 2. As expected, the ANOVA results show that observers' performance was different between adaptation conditions ($F(1.46, 45) = 131.94$, $BF_M = 2.51 \times 10^{22}$). Pairwise directional comparisons suggested that observers perceived targets to grow after receding motion adaptation (mean difference: –0.097 ± 0.061 log scaling; $t(58) = 12.15$, $BF_{+0} = 8.31 \times 10^{14}$; Figure 4A) and to shrink after looming motion adaptation (mean difference: 0.139 ± 0.080 log scaling; $t(31) = -10.26$, $BF_{-0} = 1.06 \times 10^{9}$; Figure 4B). On average, the physical target needed to shrink by ∼23% for the perceived growth to be cancelled out and to grow by ∼44% for the perceived shrinking effect to be cancelled out. There was also a robust difference in the observed mean perceived size between the receding and looming-adapted conditions ($t(31) = -12.86$, $BF_{-0} = 2.26 \times 10^{11}$). Figures 4C,D plots individual susceptibility to motion adaptation against individual differences in acuity change from adaptation (measured in Experiment 1). The plot indicates that our experiment did not reveal any significant relationship between perceived size change and acuity change from receding ($r(59) = 0.02$, $BF_{10} = 0.17$; Figure 4C) and looming ($r(32) = –0.18$, $BF_{10} = 0.35$; Figure 4D) motion adaptation. Thus, our data provides evidence that there is no relationship between acuity change and perceived size change following motion adaptation.

Consistent with the results from Experiment 1 (that adaptation to looming motion does not make acuity poorer), this result indicates that the acuity changes cannot be determined wholly by perceived size change. Therefore, while targets appear to substantially grow after receding motion adaptation and are easier to identify, they do not seem to be easier to identify because they appear larger. Furthermore, targets also appear much smaller after looming motion adaptation, but this does not impair recognition and in fact may make them somewhat easier to identify.

Experiment 3: Quantifying the role of fixation stability and pupil size

If not the perceived size, then what could produce these changes in acuity after motion adaptation? In Experiment 3, we sought to ascertain if acuity improvement could instead result from changes in fixational eye movements (stability and ocular drift) or from changes in pupil diameter, following adaptation to motion. The procedure was similar to Experiment 1—we measured acuity in observers who were either unadapted or had adapted to receding motion—but we simultaneously measured fixation stability and pupil size using infrared eye tracking. If acuity changes are reliant on changes in pupil size, changes in pupil diameter should correlate with individuals' acuity change following motion adaptation. This predicts that, for example, individuals showing the most pupil constriction will also show the greatest improvements

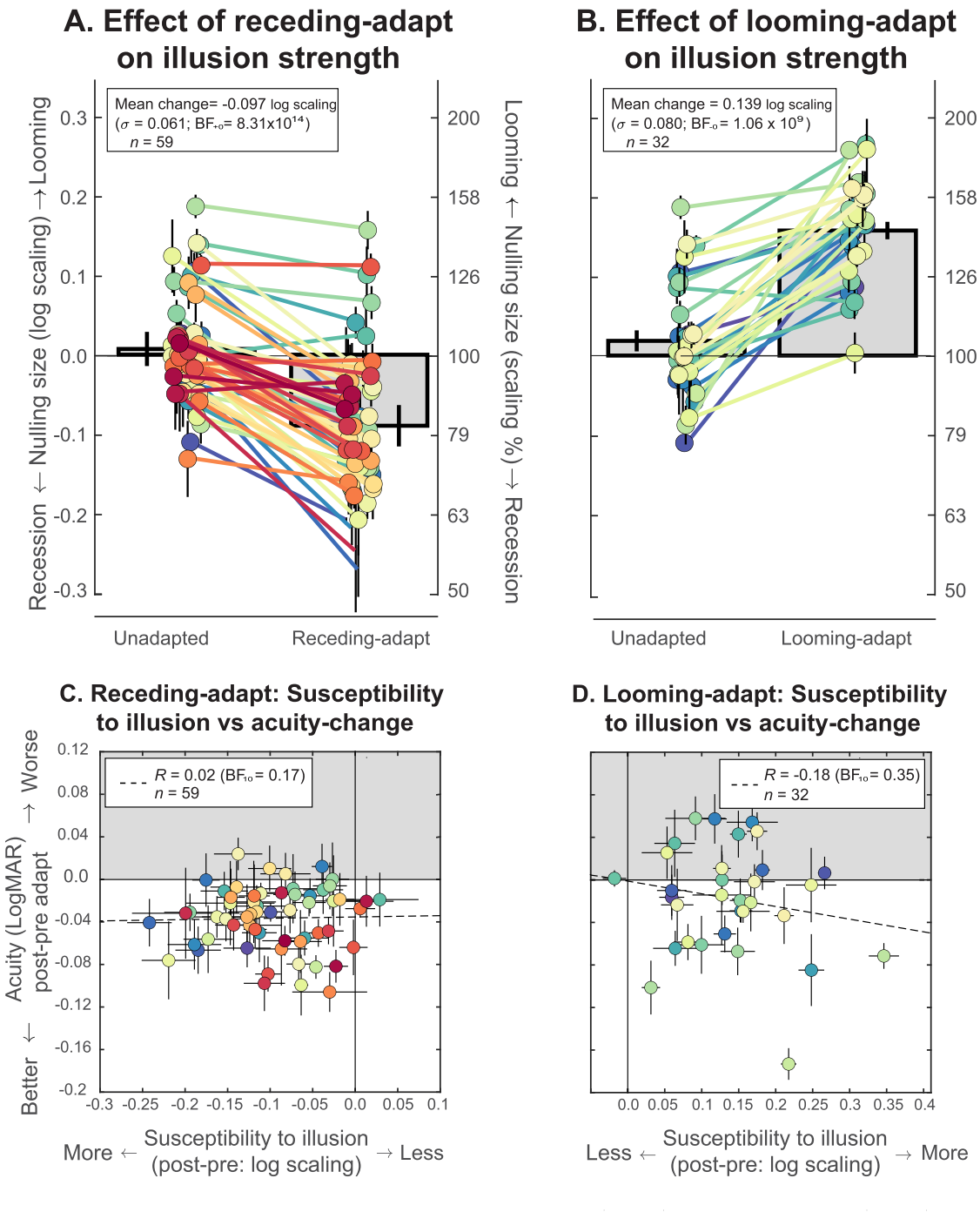

Figure 4. (A, B) Strength of the illusory motion aftereffect quantified using nulling. (A) Following adaptation to receding motion, targets needed to be physically shrunk by about 23% for observers to be equally likely to report that they shrank or grew. (B) Following adaptation to looming motion targets needed to be physically grown by about 44% for observers to be equally likely to report that they shrank or grew. The vertical axis represents the amount of physical scaling of the target sequence required for it to null the effect of adaptation. The scaling is expressed as (left axis) $\log_{10}(S)$, where $S = 1.0$ represents no scaling, or (right axis) scaling as a percentage of the size of the first symbol in the sequence. (C, D) Our data did not reveal any significant evidence of associations between susceptibility to the motion aftereffect (quantified as the nulling size change) and the change in crowded letter acuity following adaptation.

in acuity after adaptation. Similarly, if acuity changes are based on changes in fixation after adaptation, some measures of fixation should correlate with acuity change following motion adaptation. Based on the literature, we might expect higher fixation stability, increased drift curvature, reduced drift speed, and reduced drift distance to be associated with better acuity.

Methods

We recruited 30 observers (17 males, 13 females) aged 19–52 years (mean ± SD: 27 ± 9) from the University of Auckland staff and student body, 14 of whom had participated in Experiments 1 and 2.

The experimental protocol was generally similar to Experiment 1 (4AFC, 35 trials, QUEST staircases converging on 62% correct performance, all targets crowded). The differences were that we only tested receding motion adaptation and unadapted conditions, and we simultaneously measured fixation stability and pupil diameter while observers performed the task.

In terms of data analysis, we checked whether data (individual eye-tracking estimates) were normally distributed and log transformed data sets that were not. We relied on *t* tests to assess whether conditions (specified for each comparison below) impacted participants' performance. The use of Bayesian inference enabled us to quantify the evidence that our data provide in support of either the null or alternative hypotheses. Since we were interested in what variables were associated with changes in visual acuity, we also quantified the strength of associations between acuity change and the change in other metrics by computing the Pearson correlation coefficient for the relationship.

Gaze location and pupil diameter were measured using a remote near-infrared eye tracker: Tobii 4C (Gibaldi, Vanegas, Bex, & Maiello, 2017), which was mounted on a tripod 65 cm from the observers. An infrared occluder was used to occlude observers' nondominant eye. The device was then calibrated using the Tobii calibration system. Following calibration, the eye tracker continuously recorded observers' eye movements and pupil diameter at a sampling rate of 90 Hz while they performed the acuity task.

For each run of the experiment, the first 567 ms (34 frames) of data sampled by the eye-tracking device were discounted because these would have been collected when the observer was in the process of locating and fixating the centrally presented fixation dot on the screen. Before analysis, blinks were identified as samples in which eye position data were missing. Any trial that appeared to include a blink at the start or end of the trial or where more than 25% of the gaze position estimates were affected by blinks was discounted. Only fixation estimates that were sampled during the time the target stimulus was displayed on the screen (1.5 s) were analyzed and broken into a series of sequences punctuated by blinks. The x and y eye-position data within each sequence was smoothed using a third-order, low-pass Savitzky Golay polynomial filter (Savitzky & Golay, 1964). We calculated eye movement speed as the product of the difference between two consecutive gaze positions and the sampling frequency of the eye-tracking device. We used the speed estimates to separate gaze position estimates into sequences of drift (eye movements with speed <10 deg/s) and microsaccades (eye movements with speed >10 deg/s).

Fixation stability was estimated with a bivariate contour ellipse area (BCEA) formula (Crossland, Sims, Galbraith, & Rubin, 2004), which estimates the area of the ellipse that encompasses a given proportion of the gaze position data:

$$\mathrm{BCEA} = 2k\pi\sigma_H\sigma_V\sqrt{1-\rho^2}, \qquad (2)$$

where σ_H and σ_V are the standard deviations of gaze point locations over the X and Y dimensions, respectively, and ρ is the product–moment correlation of X and Y positions. k is a constant and can be derived from

$$P = 1 - e^{-k}, \quad (3)$$

where P is the probability that fixation points will lie within the ellipse and e is the natural logarithm. We used a k value of 1.14 corresponding to a probability (P) value of 0.68. This value is consistent with previous research (Crossland, Sims, Galbraith, & Rubin, 2004). Mean BCEA was estimated for each trial separately and then averaged across all trials for all runs for each condition and observer. As part of BCEA calculation, the product–moment correlation between the x and y coordinates of gaze position data and the standard deviation for data in each direction were estimated. Mean pupil diameter estimates were also obtained for each trial and averaged across all trials for all runs for each condition and observer.

In a further analysis of the fixation data, the curvature of drift eye movements was estimated (Intoy & Rucci, 2020). In this analysis, the sequence of drift eye positions was plotted and the angular difference between consecutive eye positions was calculated using the MATLAB function "angdiff" after the angular sequence between adjacent points was estimated. Drift curvature was determined as the absolute value of the angular subtense between adjacent gaze positions while drift distance was calculated as the total distance traversed by the eye in the course of a trial. All measurements were estimated for each trial and averaged across trials for all runs in a given condition and for each observer.

Results

Broadly replicating results from Experiment 1, we found strong evidence of an improvement in visual acuity (mean change: –0.035 ± 0.048 LogMAR, $t(29) = 4.032$, $BF_{+0} = 161.66$) for receding motion-adapted compared to unadapted viewing conditions.

We found that fixation stability was not associated with better acuity after adaptation ($r(30) = 0.38$, $BF_{10} = 1.80$; Figure 5B). Moreover, we found strong supporting evidence showing that fixation stability does not improve following adaptation to receding motion (mean change = 0.25 ± 0.062 deg^2, $t(29) = –2.1$, $BF_{+0} = 0.069$; Figure 5A), suggesting minimal effect of fixation stability. These results therefore argue against any mechanistic association between these factors. Similarly, observers' pupil size remained relatively consistent across conditions. Crucially, we show that there is no difference in pupil size before and following receding motion adaptation with Bayesian evidence moderately in favor of the null hypothesis (unadapted: 4.61 ± 0.71 mm, receding motion adapted: 4.62 ± 0.71 mm, mean change = 0.009 ± 0.25 mm, $t(29) = –0.20$, $BF_{+0} = 0.17$; Figure 5C). There was also no evidence for a link between change in pupil size and acuity change following motion adaptation ($r(30) = 0.28$, $BF_{10} = 0.68$; Figure 5D).

Further analyses also revealed consistent drift fixation patterns between the unadapted and the motion-adapted conditions. Neither curvature of ocular drift (unadapted: 1.51 ± 0.076 deg, adapted: 1.49 ± 0.10 deg, mean difference –0.020 deg, $t(29) = 1.5$, $BF_{+0} = 0.93$), drift speed (unadapted: 6.94 ± 2.30 deg/s, adapted: 7.76 ± 3.38 deg/s, mean difference = 0.82 deg/s, $t(29) = –1.8$, $BF_{+0} = 0.077$), nor drift distance (unadapted: 89.75 ± 33.38 deg, adapted: 114.65 ± 82.38 deg, mean difference = 24.90 deg, $t(29) = –1.9$, $BF_{+0} = 0.073$) differed between the unadapted and receding motion-adapted conditions. Further, none of these metrics were associated with change in acuity (drift curvature $r(30) = –0.15$, $BF_{10} = 0.31$; drift speed: $r(30) = 0.15$, $BF_{10} = 0.30$; and drift distance: $r(30) = 0.19$, $BF_{10} = 0.38$).

Taken together, our results do not support the idea that fixational eye movements or pupil size account for motion adaptation-induced acuity change.

Discussion

Acuity changes are not the result of changes in perceived size

We confirmed that modest but reliable changes in acuity—typically around two letters on an eye chart—occur following adaptation to receding motion. Counter to our hypothesis, looming motion adaption did not impair acuity. The acuity gains we observe are unlikely to be due to changes in overall perceived size of the stimulus, which we note will modify both the perceived target size and the spacing of target and crowding flankers. Two lines of evidence support this conclusion.

Looming adaptation causes targets to appear smaller but not harder to identify

Looming motion adaptation generates a contracting motion aftereffect, causing targets to appear substantially smaller. We confirmed that this was a robust change using our nulling paradigm (Experiment 2) where we observe twice as much shrinking with looming adaptation than growth with receding adaptation. That acuity subtly *improves* after such adaptation is contrary both to the notion that perceived size drives acuity change and to the conclusions of Experiment 1 reported in Lages et al. (2017). We note, however, that the earlier experiment was compromised by ceiling effects—arising from the use of a nonadaptive procedure—leading the authors to have to split participants into low- and high-achieving groups, for the purpose of analyzing results at a group level. To address this issue, in their Experiment 2, Lages et al. (2017) used an adaptive procedure to avoid such ceiling effects, and under these conditions—although authors do not comment on it—their results are similar to our own. Essentially, receding motion adaptation improves acuity and looming motion adaptation does not impair acuity (reanalysis of raw data from https://osf.io/nav9h/; mean acuity change, receding adaptation: –0.019 LogMAR, $t(31) = 3.12$, $BF_{+0} = 19.83$; mean acuity change, looming adaptation: –0.017 LogMAR, $t(31) = 4.31$, $BF_{-0} = 0.043$). Thus, we see no contradiction between our own results and those from Experiment 2 reported in the earlier study.

Further, we consider it unlikely that we failed to measure *acuity loss* because of any intrinsic limitation of our procedure. By changing target orientation during presentation, we constrained measurement of performance to the time when perceived size change was most pronounced. This procedure offers the opportunity for maximum *disruption* of recognition following adaptation.

Susceptibility to motion adaptation is not associated with greater changes in acuity

Experiment 2 explored the influence of individual differences in perceived size following adaptation on individual differences in acuity gain observed in Experiment 1 by quantifying observers' susceptibility to motion adaptation using a *nulling paradigm*. We

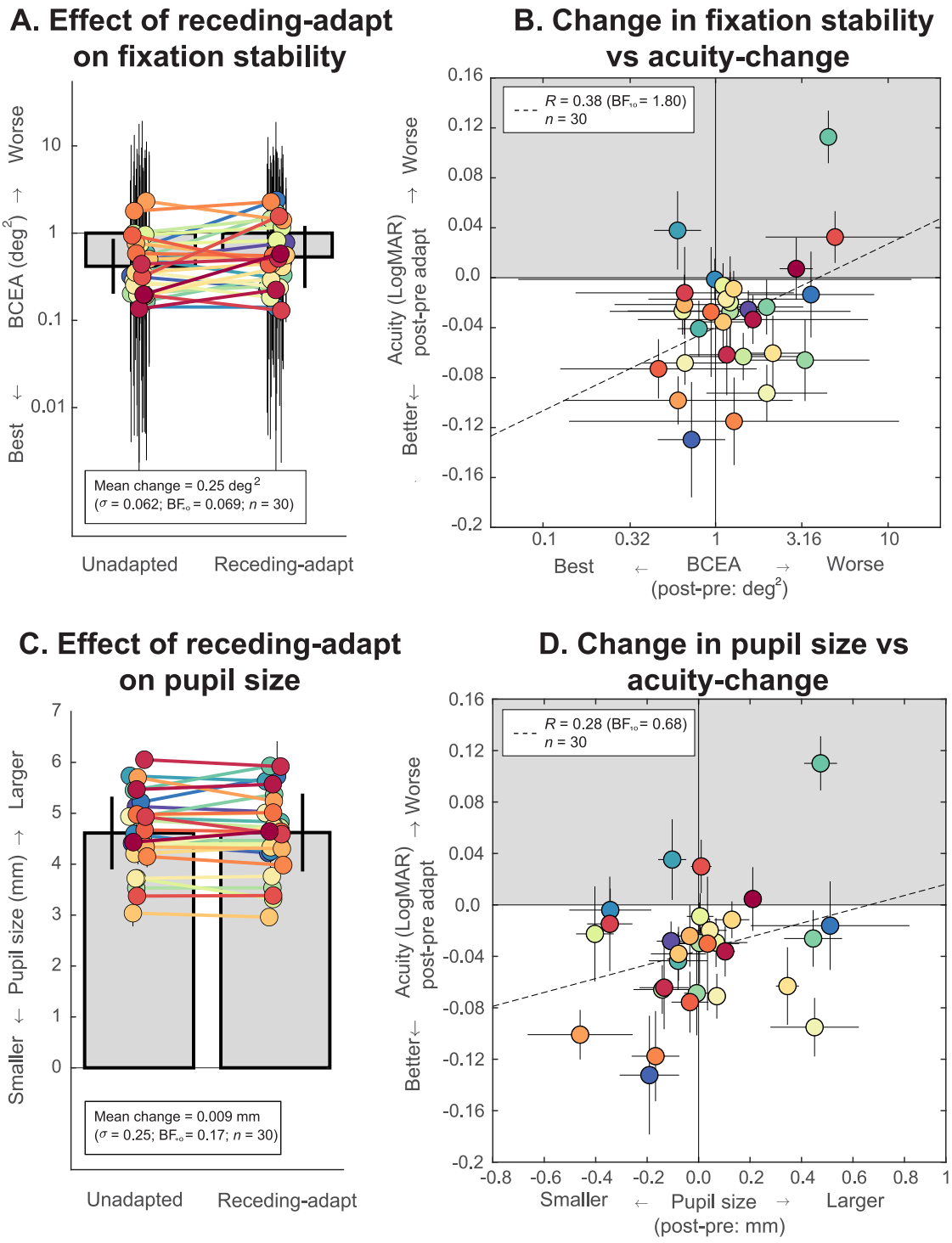

Figure 5. Association between acuity change and (A, B) fixation stability or (C, D) pupil size. (A) Comparison of observers' BCEA following either no motion adaptation or receding motion adaptation. Each solid disc represents average data for each individual, and error bars represent ±1 *SEM*. We observe significantly poorer fixation stability following adaptation. (B) Fixation stability was not associated with substantially better acuity outcomes. (C) Comparison of pupil size following either unadapted or receding motion adaptation. Pupil size remained unchanged and (D) showed no significant link with acuity change. We found no evidence in support of the hypotheses that fixational eye movements and pupil size account for motion adaptation-induced gains in visual acuity.

reasoned that observers who are more susceptible to adaptation should show more change in perceived size, which—if perceived size determines acuity—in turn should translate into greater acuity gains. To test this idea, we measured the strength of physical motion/size change required to null the illusory motion induced by adaptation, as a proxy measure for individual susceptibility to perceived size change following adaptation. In line with our expectation, observers' nulling performance was consistent with their perceiving substantial growth of targets following receding motion adaptation and considerable shrinking of targets following looming motion adaptation.

Despite the magnitude of these effects and the range of effect sizes observed, *individual observers' susceptibility to adaptation did not correlate with their measured acuity change*. This supports a dissociation between perceived size and acuity change, although we note our use of nulling (rather than size matching) potentially complicates the interpretation. Specifically, there may be distinct components of the perception of a target following motion adaptation: (1) motion (receding or looming), (2) size change (the sense of shrinking or growth of the target over time), and (3) perceived size (subjective magnification or minification of the target). Although each component may influence acuity, the judgment of target orientation (Experiments 1 and 3) likely depends most on *perceived size*. On the other hand, in measuring susceptibility to motion adaptation (Experiment 2), the physical target motion is specifically designed to cancel out all three perceptual components induced by motion adaptation. In this task, observers are asked to make a judgment closely related to *size change*: "Is the target growing or shrinking?" It is possible that the relative reliance on perceived size (for acuity) versus size change (for susceptibility) could account for the dissociation between acuity and susceptibility to motion adaptation. In short, we have no way of knowing based on this paradigm. However, our efforts at directly measuring perceived size using matching (as outlined in the Methods) proved unworkable, since this task requires a reference to be spatially or temporally offset from the target, which can make the judgment of relative size very difficult for observers. Task difficulty is also compounded by the target appearing to change size over time following adaptation. This forces observers to make an arbitrary decision about *when* to make their matching decision. The nulling paradigm eliminates these issues.

We note another line of evidence demonstrating that perceived size enhances visual sensitivity from Schindel and Arnold (2010). They showed that they could influence perceived size of a Gabor target by manipulating its *apparent* viewing distance (through the use of vergence cues in a stereo display). The Gabor appeared larger when seen as being far or smaller when seen as being near. It was the perceived size of the target that determined how well participants could judge its orientation (with apparently larger objects being easier). This effect did not extend to contrast sensitivity (CS), which the authors judge to be consistent with findings that CS is limited by the area of V1 stimulated, which is in turn constant for an image of fixed retinal size (Murray, Boyaci, & Kersten, 2006). The authors conclude that the critical difference for their orientation task related to "*judgements concerning clearly visible stimulus properties*," which were susceptible to the influence of illusory size change. In our experiment, observers performed an acuity task with a target stimulus (tumbling T), for which the critical property is the relative location of the two bars comprising the optotype. Unlike the clearly visible critical detail in the orientation task used by Schindel and Arnold, relative location information in our stimulus is not clearly visible at threshold. As such, our task is more akin to Schindel and Arnold's contrast sensitivity task, and our finding a lack of influence of perceived size is consistent with their findings.

Crowding is insufficient to explain changes in acuity

All targets presented following adaptation were crowded by flanking optotypes. If we consider the effect of adaptation on the size of the *overall stimulus* (i.e., target and flankers), it is possible that gains in acuity arise not from changes in target size but from changes in the perceived spacing of flanker and target, which could produce some "knock-on" reduction in foveal crowding. However, the reported magnitude of crowding (the difference in acuity for flanked letters and for isolated letters) was less than typical gains in acuity achieved through adaptation (Experiment 1), and it is therefore logically impossible for these gains to originate wholly from a reduction in crowding. It is important to note that our foveal crowding ratio (the ratio of isolated to flanked letter acuity) was only 1.02, a modest effect compared to ratios reported elsewhere—typically around 1.12 (Huurneman et al., 2012; Pardhan, 1997). The differences could be attributable to various factors, including target-flanker spacing, the type of targets/flankers used, and the number of flanking elements. Crowding may have been amplified if we had used more complex targets (such as Sloan letters; Pardhan, 1997), spaced target and flankers more closely (0.4-letter gap; Coates, Levi, Touch, & Sabesan, 2018), or more flanking elements (Pardhan, 1997). Nevertheless, and quite fundamentally, since we still report robust improvements in acuity, in a task that does not elicit strong crowding, it is unlikely that the benefit in acuity from motion adaptation arises from a reduction in crowding (a conclusion also drawn by Lages, Boyle, & Jenkins, 2017) or, by

extension, from an illusory increase in target-flanker spacing accompanying an overall increase in perceived size.

Acuity changes are not due to pupil size or eye movements

Since pupil size can benefit or impair visual acuity (Atchison, Smith, & Efron, 1979), we wondered if our acuity gains could originate from a change in pupil size arising from motion adaptation. Assuming a baseline pupil size of 4.5 mm, pupil size would have to nearly halve (Atchison, Smith, & Efron, 1979) to produce the modest acuity benefit we report in Experiments 1 and 3. Contrary to this, we report negligible pupil size change following motion adaptation. Consistent with previous findings (Lages, Boyle, & Jenkins, 2017), expanding and contracting motion aftereffects are unlikely to be changing pupil size in a way that accounts for measured acuity changes.

In terms of ocular drift, Intoy and Rucci (2020) showed that performance of fine acuity tasks leads to a reduction in the total distance traveled by the eye. During their stimulus presentation, eye movements become slower and more curved (Intoy & Rucci, 2020). However, our data are not consistent with adaptation changing any of a range of metrics quantifying the speed, distance covered, or curvature or participants' eye movements. Although our hardware did not support making measurements with the precision of Rucci's group, we note that the effects they reported were very large. On average, there was a ∼63% decrease in drift distance, a 15% reduction in drift speed, and about a 27% increase in drift curvature when observers performed a high-acuity task. Were such effects to be having a knock-on influence on acuity in our study, then we would anticipate them being measurable with infrared eye-tracking hardware. The absence of measured association between acuity gain and these metrics quantifying eye movements makes it unlikely that changes in eye movements support acuity improvements.

Together, neither pupil size, fixation stability, nor metrics associated with ocular drift were associated with motion adaptation-induced changes in acuity.

What is driving acuity gains after motion adaptation?

Role for a direction-independent mechanism, such as blur adaptation

Could acuity changes from motion adaptation be explained by changes in the sensitivity of spatial-frequency (SF) tuned channels (Campbell & Robson, 1968), as has been used to account for findings from more established paradigms such as blur adaptation (Mon-Williams et al., 1998; Rajeev & Metha, 2010) and flicker adaptation (Arnold, Williams, Phipps, & Goodale, 2016), which have both been shown to improve high-contrast letter acuity (Arnold, Williams, Phipps, & Goodale, 2016; Mon-Williams et al., 1998; Rajeev & Metha, 2010)? In particular, it has been reported that although blur adaptation reduces sensitivity to low and mid-SFs (Mon-Williams et al., 1998; Rajeev & Metha, 2010) (as might be expected), adaptation can be accompanied by an enhancement in sensitivity for high SF grating patches (Rajeev & Metha, 2010). Such a modulation of sensitivity in SF-tuned channels is thought to be a form of "gain control" aimed at compensating for optical and neural blur in order to maintain contrast constancy (Georgeson & Sullivan, 1975) (i.e., near-veridical perceived contrast of gratings of different SFs, despite varying contrast sensitivity). Such a mechanism could be similar to "deblurring" or "sharpening" since it can serve to reduce the influence of the higher-sensitivity lower SF-tuned channels on the perception of contrast in broadband patterns (that contain a range of SFs), improving the "clarity" of vision (Georgeson & Sullivan, 1975). We suggest it may also serve to actively improve sensitivity to higher SF structure in SF broadband patterns (like letters). This is essentially identical to Arnold et al.'s (2016) suggestion that when coarse-scale spatiotemporal information signaled by the magnocellular pathway is suppressed, then sensitivity to fine-scale structure (signaled by the parvocellular pathway) is enhanced. This, they argue, explains why adaptation to flicker, which likely suppresses operation of the magnocellular visual pathway (a) reduces contrast sensitivity for low but not high narrowband SF targets and (b) can lead to a transient enhancement in spatial acuity for a broadband target. Both findings are consistent with the unadapted parvocellular signals being either respectively (a) unaffected or (b) released from suppression as a result of adaptation.

Could it be a bit of both?

If the mechanism of acuity change is wholly direction independent, and both receding and looming motion adaptation improve acuity in similar ways to blur and flicker adaptation, then why did we not observe the same effect on acuity of looming compared to receding adaptation? First of all, we report only weak statistical evidence for a difference in acuity gains between these conditions. We note that our reanalysis of data from Lages et al. (2017) (Section 1 of Discussion) suggests a very similar acuity gain for both motion directions. Further, we speculate that the benefit we observe in both conditions could arise from the combination of two effects: (1) a direction-independent acuity gain

resulting from enhanced sensitivity to fine spatial structure as a result of motion adaptation (discussed in the previous section) and (2) acuity changes based on perceived size changes, partially through modest changes in crowding. Such a combination between these two main effects could potentially account for the main pattern of our results. Receding motion adaptation would lead to improved acuity based on both proposed mechanisms, whereas looming motion adaptation would be influenced by acuity increases (from direction-independent enhanced sensitivity to fine spatial structure) and decreases (from perceptual shrinking). Because the result (acuity) is a combination of these two effects, we would expect looming motion adaptation to lead to weaker acuity gains than receding. This could also explain why we did not find dependence of acuity change on susceptibility to crowding or adaptation.

Conclusion

We have shown that visual acuity improves following adaptation to receding and looming motion. Our results are unlikely to be explicable by changes in eye movements or pupil size or to result wholly from changes in perceived target size and/or associated reductions in crowding. We conclude that our main finding (acuity gain from motion adaptation) and a range of related effects likely result from changes in gain control of visual channels tuned for coarse-scale information, improving information transmission through channels tuned for fine-scale information.

Keywords: acuity, adaptation, motion aftereffect, fixation stability, pupil size

Acknowledgments

The authors thank Soheil M. Doustkouhi for suggesting the nulling paradigm. We also thank Catherine Morgan, Tony Han, and Aryaman Taore for their input. This research was supported by a Marsden research grant (grant number: 3716355), New Zealand.

In line with open science practices, data from this project are made available on the open science framework (OSF) via this link: https://osf.io/cy5jk/.

Commercial relationships: none.
Corresponding author: Steven C. Dakin.
Email: s.dakin@auckland.ac.nz.
Address: School of Optometry and Vision Science, Faculty of Medical & Health Sciences, The University of Auckland, Auckland, New Zealand.

Footnote

[1]The slightly higher value of 2.2 letters reported in Lages et al. (2017) is a result of their performing a median split on their results—based on unadapted acuity—which increased their effect size.

References

Anstis, S., Verstraten, F. A. J., & Mather, G. (1998). The motion aftereffect. *Trends in Cognitive Sciences, 2*(3), 111–117.

Arnold, D. H., Williams, J. D., Phipps, N. E., & Goodale, M. A. (2016). Sharpening vision by adapting to flicker. *Proceedings of the National Academy of Sciences of the United States of America, 113*(44), 12556–12561.

Atchison, D. A., Smith, G., & Efron, N. (1979). The effect of pupil size on visual acuity in uncorrected and corrected myopia. *American Journal of Optometry and Physiological Optics, 56*(5), 315–323.

Beatty, J., & Wagoner, B. L. (1978). Pupillometric signs of brain activation vary with level of cognitive processing. *Science, 199*(4334), 1216–1218.

Beukema, S., Olson, J. A., & Jennings, B. J. (2017). Pupil dilation to illusory motion in peripheral drift images: Perception versus reality. *Journal of Vision, 17*(8), 1.

Bex, P. J., Metha, A. B., & Makous, W. (1999). Enhanced motion aftereffect for complex motions. *Vision Research, 39*(13), 2229–2238.

Bouma, H. (1970). Interaction effects in parafoveal letter recognition. *Nature, 226*(5241), 177–178.

Boynton, G. M., & Duncan, R. O. (2002). Visual acuity correlates with cortical magnification factors in human V1. *Journal of Vision, 2*(10), 11.

Brainard, D. H. (1997). The Psychophysics Toolbox. *Spatial Vision, 10*(4), 433–436.

Campbell, F. W., & Green, D. G.. (1965). Optical and retinal factors affecting visual resolution. *Journal of Physiology, 181*(3), 576–593.

Campbell, F., & Gubisch, R. (1966). Optical quality of the human eye. *Journal of Physiology, 186*(3), 558–578.

Campbell, F. W., & Robson, J. G. (1968). Application of Fourier analysis to the visibility of gratings. *Journal of Physiology, 197*(3), 551–566.

Castellotti, S., Francisci, C., & Del Viva, M. M. (2021). Pupillary response to real, illusory, and implied motion. *PLoS One, 16*(7), e0254105.

Coates, D. R., Levi, D. M., Touch, P., & Sabesan, R. (2018). Foveal crowding resolved. *Scientific Reports, 8*(1), 9177.

Connolly, M., & Van Essen, D. (1984). The representation of the visual field in parvicellular and magnocellular layers of the lateral geniculate nucleus in the macaque monkey. *Journal of Comparative Neurology, 226*(4), 544–564.

Cowey, A., & Rolls, E. T. (1974). Human cortical magnification factor and its relation to visual acuity. *Experimental Brain Research, 21*(5), 447–454.

Crossland, M. D., Sims, M., Galbraith, R. F., & Rubin, G. S. (2004). Evaluation of a new quantitative technique to assess the number and extent of preferred retinal loci in macular disease. *Vision Research, 44*(13), 1537–1546.

Curcio, C. A., & Allen, K. A. (1990). Topography of ganglion cells in human retina. *Journal of Comparative Neurology, 300*(1), 5–25.

Curcio, C. A., Sloan, K. R., Kalina, R. E., & Hendrickson, A. E. (1987). Human photoreceptor topography. *Journal of Comparative Neurology, 292*, 497–523.

Dacey, D. M. (1993). The mosaic of midget ganglion cells in the human retina. *Journal of Neuroscience, 13*(12), 5334–5355.

Dakin, S. C., Cass, J., Greenwood, J. A., & Bex, P. J. (2010). Probabilistic, positional averaging predicts object-level crowding effects with letter-like stimuli. *Journal of Vision, 10*(10), 14.

Dakin, S. C., Greenwood, J. A., Carlson, T. A., & Bex, P. J. (2011). Crowding is tuned for perceived (not physical) location. *Journal of Vision, 11*(9), 1–13.

Dow, B., Snyder, A., Vautin, R., & Bauer, R. (1981). Magnification factor and receptive field size in foveal striate cortex of the monkey. *Experimental Brain Research, 44*(2), 213–228.

Fang, F., Boyaci, H., Kersten, D., & Murray, S. O. (2008). Attention-dependent representation of a size illusion in human V1. *Current Biology, 18*(21), 1707–1712.

Freeman, J., & Simoncelli, E. P. (2011). Metamers of the ventral stream. *Nature Neuroscience, 14*(9), 1195–1201.

Georgeson, M. A., & Sullivan, G. D. (1975). Contrast constancy: Deblurring in human vision by spatial frequency channels. *Journal of Physiology, 252*(3), 627–656.

Gibaldi, A., Vanegas, M., Bex, P. J., & Maiello, G. (2017). Evaluation of the Tobii EyeX Eye tracking controller and Matlab toolkit for research. *Behavior Research Methods, 49*(3), 923–946.

Hamm, L. M., Yeoman, J. P., Anstice, N., & Dakin, S. C. (2018). The Auckland Optotypes: An open-access pictogram set for measuring recognition acuity. *Journal of Vision, 18*(3), 13.

Hou, C., Kim, Y.-J., & Verghese, P. (2017). Cortical sources of Vernier acuity in the human visual system: An EEG-source imaging study. *Journal of Vision, 17*(6), 2.

Huurneman, B., Boonstra, F. N., Cox, R. F., Cillessen, A. H., & Van Rens, G. (2012). A systematic review on 'foveal crowding' in visually impaired children and perceptual learning as a method to reduce crowding. *BMC Ophthalmology, 12*(1), 1–14.

Intoy, J., & Rucci, M. (2020). Finely tuned eye movements enhance visual acuity. *Nature Communications, 11*(1), 795.

Jackson, A., & Bailey, I. (2004). Visual acuity. *Optometry in Practice, 5*, 53–70.

JASP Team (2022). Version 0.16.3 [Computer software].

Kolb, H., Linberg, K. A., & Fisher, S. K. (1992). Neurons of the human retina: A Golgi study. *Journal of Comparative Neurology, 318*(2), 147–187.

Lages, M., Boyle, S. C., & Jenkins, R. (2017). Illusory increases in font size improve letter recognition. *Psychological Science, 28*(8), 1180–1188.

Levi, D. M. (2008). Crowding—an essential bottleneck for object recognition: A mini-review. *Vision Research, 48*(5), 635–654.

Levi, D., Klein, S., & Hariharan Vilupuru, S. (2002). Suppressive and facilitatory spatial interactions in foveal vision: Foveal crowding is simple contrast masking. *Journal of Vision, 2*, 140–166.

Levi, D. M., Klein, S. A., & Aitsebaomo, A. (1985). Vernier acuity, crowding and cortical magnification. *Vision Research, 25*(7), 963–977.

Levi, D. M., Klein, S. A., & Carney, T. (2000). Unmasking the mechanisms for Vernier acuity: Evidence for a template model for Vernier acuity. *Vision Research, 40*(8), 951–972.

Mon-Williams, M., Tresilian, J. R., Strang, N. C., Kochhar, P., & Wann, J. P. (1998). Improving vision: Neural compensation for optical defocus. *Proceedings: Biological Sciences, 265*(1390), 71–77.

Murray, S. O., Boyaci, H., & Kersten, D. (2006). The representation of perceived angular size in human primary visual cortex. *Nature Neuroscience, 9*(3), 429–434.

O'Brien, B. (1951). Vision and resolution in the central retina. *Journal of the Optical Society of America, 41*(12), 882–894.

Packer, O., & Williams, D. R. (1992). Blurring by fixational eye movements. *Vision Research, 32*(10), 1931–1939.

Pardhan, S. (1997). Crowding in visually impaired patients: contour interaction and/or gaze-selection defects? *Neuro-Ophthalmology, 18*(2), 59–65.

Perry, V. H., & Cowey, A. (1985). The ganglion cell and cone distribution in the monkey's retina: Implications for central magnification factors. *Vision Research, 12*, 1795–1810.

Rajeev, N., & Metha, A. (2010). Enhanced contrast sensitivity confirms active compensation in blur adaptation. *Investigative Ophthalmology & Visual Science, 51*(2), 1242–1246.

Sahraie, A., & Barbur, J. L. (1997). Pupil response triggered by the onset of coherent motion. *Graefe's Archive for Clinical and Experimental Ophthalmology, 235*(8), 494–500.

Salmon, T. O., & van de Pol, C. (2006). Normal-eye Zernike coefficients and root-mean-square wavefront errors. *Journal of Cataract & Refractive Surgery, 32*(12), 2064–2074.

Savitzky, A., & Golay, M. J. (1964). Smoothing and differentiation of data by simplified least squares procedures. *Analytical Chemistry, 36*(8), 1627–1639.

Schindel, R., & Arnold, D. H. (2010). Visual sensitivity can scale with illusory size changes. *Current Biology, 20*(9), 841–844.

Schwarzkopf, D. S., & Rees, G. (2013). Subjective size perception depends on central visual cortical magnification in human V1. *PLoS One, 8*(3), e60550.

Schwarzkopf, D. S., Song, C., & Rees, G. (2011). The surface area of human V1 predicts the subjective experience of object size. *Nature Neuroscience, 14*(1), 28–30.

Shannon, C. E. (1948). A mathematical theory of communication. *The Bell System Technical Journal, 27*(3), 379–423.

Smith, A. T., Singh, K. D., Williams, A. L., & Greenlee, M. W. (2001). Estimating receptive field size from fMRI data in human striate and extrastriate visual cortex. *Cerebral Cortex, 11*(12), 1182–1190.

Snyder, A. W., & Miller, W. H. (1977). Photoreceptor diameter and spacing for highest resolving power. *Journal of the Optical Society of America A, 67*(5), 696–698.

Song, C., Schwarzkopf, D. S., Kanai, R., & Rees, G. (2015). Neural population tuning links visual cortical anatomy to human visual perception. *Neuron, 85*(3), 641–656.

Song, C., Schwarzkopf, D. S., & Rees, G. (2013). Variability in visual cortex size reflects tradeoff between local orientation sensitivity and global orientation modulation. *Nature Communications, 4*(1), 1–10.

Steinman, R. M., & Levinson, J. Z. (1990). The role of eye movement in the detection of contrast and spatial detail. *Eye Movements and Their Role in Visual and Cognitive Processes, 4*, 115–212.

Tarita-Nistor, L., González, E. G., Mandelcorn, M. S., Lillakas, L., & Steinbach, M. J. (2009). Fixation stability, fixation location, and visual acuity after successful macular hole surgery. *Investigative Ophthalmology & Visual Science, 50*(1), 84–89.

Thibos, L., Walsh, D., & Cheney, F. (1987). Vision beyond the resolution limit: Aliasing in the periphery. *Vision Research, 27*(12), 2193–2197.

Thibos, L. N., & Bradley, A. (1993). New methods for discriminating neural and optical losses of vision. *Optometry and Vision Science, 70*(4), 279–287.

Thibos, L. N., Bradley, A., Still, D. L., Zhang, X., & Howarth, P. A. (1990). Theory and measurement of ocular chromatic aberration. *Vision Research, 30*(1), 33–49.

Thibos, L. N., Hong, X., Bradley, A., & Cheng, X. (2002). Statistical variation of aberration structure and image quality in a normal population of healthy eyes. *Journal of the Optical Society of America A, 19*(12), 2329–2348.

van Doorn, J., van den Bergh, D., Böhm, U., Dablander, F., Derks, K., Draws, T., . . . Wagenmakers, E.-J. (2021). The JASP guidelines for conducting and reporting a Bayesian analysis. *Psychonomic Bulletin & Review, 28*(3), 813–826.

Villegas, E. A., Alcón, E., & Artal, P. (2008). Optical quality of the eye in subjects with normal and excellent visual acuity. *Investigative Ophthalmology & Visual Science, 49*(10), 4688–4696.

Virsu, V., Näsänen, R., & Osmoviita, K. (1987). Cortical magnification and peripheral vision. *Journal of the Optical Society of America A, 4*(8), 1568–1578.

Watson, A. B. (2014). A formula for human retinal ganglion cell receptive field density as a function of visual field location. *Journal of Vision, 14*(7), 15.

Watson, A. B., & Pelli, D. G. (1983). Quest: A Bayesian adaptive psychometric method. *Perception & Psychophysics, 33*(2), 113–120.

Waugh, S. J., Levi, D. M., & Carney, T. (1993). Orientation, masking, and vernier acuity for line targets. *Vision Research, 33*(12), 1619–1638.

Wells-Gray, E. M., Choi, S. S., Bries, A., & Doble, N. (2016). Variation in rod and cone density from the fovea to the mid-periphery in healthy human retinas using adaptive optics scanning laser ophthalmoscopy. *Eye, 30*(8), 1135–1143.

Whitaker, D., McGraw, P. V., & Pearson, S. (1999). Non-veridical size perception of expanding and contracting objects. *Vision Research, 39*(18), 2999–3009.

Whitney, D., Goltz, H. C., Thomas, C. G., Gati, J. S., Menon, R. S., & Goodale, M. A. (2003). Flexible retinotopy: Motion-dependent position coding in the visual cortex. *Science, 302*(5646), 878–881.

Whitney, D., & Levi, D. M. (2011). Visual crowding: a fundamental limit on conscious perception and object recognition. *Trends in Cognitive Sciences, 15*(4), 160–168.

Williams, D. R. (1985). Aliasing in human foveal vision. *Vision Research, 25*(2), 195–205.

Williams, D. R. (1986). Seeing through the photoreceptor mosaic. *Trends in Neurosciences, 9*, 193–198.

Williams, D. R., & Coletta, N. J. (1987). Cone spacing and the visual resolution limit. *Journal of the Optical Society of America A, 4*(8), 1514–1523.

Wohlgemuth, A. (1911). *On the after-effect of seen movement*. Cambridge, UK: University Press.

Supplementary material

Supplementary Movie S1. A 30-s receding-motion adaptation stimulus, followed by an acuity test stimulus comprising a sequence of tumbling Ts.

Supplementary Movie S2. A 30-s receding-motion adaptation stimulus, followed by a nulling stimulus comprising a sequence of tumbling Ts that are physically receding. When the rate of physical recession matches the rate of illusory looming, the two cancel each other out and the reader should experience relatively little size change (compared to their experience with Supplementary Movie S1).